

ORIGINAL RESEARCH PAPER

Sensitivity Analysis for Stress, Heat-Treating, and Rare-Earth Elements on Fatigue Lifetime of AZ91 Magnesium Alloy

A. Yousefi Parchin Oliya^a, M. Azadi^{b,*}, M. Mokhtarishirazabad^c

^aFaculty of Aerospace Engineering, Semnan University, Semnan, Iran.

^bFaculty of Mechanical Engineering, Semnan University, Semnan, Iran.

^cDepartment of Mechanical Engineering, University of Bristol, United Kingdom.

Article info

Article history:

Received 20 November 2021

Received in revised form

01 February 2022

Accepted 08 February 2022

Keywords:

Sensitivity analysis

Magnesium alloys

Heat treatment

Rare-earth element

Fatigue lifetime

Abstract

In this article, the changes in High-Cycle Fatigue (HCF) lifetimes of the AZ91 magnesium alloy are investigated under the influences of the different heat treatments and also the Rare-Earth (RE) element addition. For this purpose, some different heat treatments, including a common solution treatment, with different ageing treatments and RE elements were performed. Then, the sensitivity analysis was done using the regression analysis by the DESIGN EXPERT software on the experimental data. At a similar fatigue lifetime, the RE element increased the strength or the stress level by at least 30%, and also, the RE element with heat-treating enhanced the material strength by at least 50%. The results of sensitivity analysis on the experimental data illustrated that the stress level, the heat treatment, and the RE element (RE) were the most effective parameters on the fatigue lifetime, respectively. Besides, the fatigue lifetime was sensitive to the interaction of the heat treatment and the RE element. In addition, the fracture surface analysis demonstrated that all samples had three different zones for the crack initiation, the crack growth, and the sudden final fracture.

1. Introduction

Magnesium alloy is called the green engineering material due to the reduction of the weight of the cars and reducing the impact of greenhouse gases [1]. The application of magnesium alloys is expanding in the aerospace and automobiles industries for various applications [2]. Its advantages include good machinability, high shock-absorbing capacity, good recycling, low density [3, 4]. On the other hand, its disadvantages are the low modulus of elasticity, weak corrosion resistance, poor formability, susceptibility to creep, and

low velocity of diffusion processes during heat treatment [5–7].

To improve these poor properties, researchers use various strengthening mechanisms. Therefore, some research is reviewed below.

Li et al. [8] analyzed the effect of heat treatment on the fatigue behavior in S-N and S-S of AZ91D alloy in different test temperatures. They claimed that the fatigue lifetime increased with decreasing grain size due to heat treatment. In addition, this alloy has shown better fatigue properties in low-temperature test environments. Khisheh et al. [9] studied the time and tem-

*Corresponding author: M. Azadi (Associate Professor)

E-mail address: m_azadi@semnan.ac.ir

<http://dx.doi.org/10.22084/jrstan.2022.25222.1199>

ISSN: 2588-2597

perature effects of aging treatments on the mechanical properties of AlSiCu alloy. They claimed that the highest values of the hardness, tensile, and yield stress were obtained after ageing at 200 °C and 3 hours. Their sensitivity analysis showed that ageing temperature was the most effective factor. Zhang et al. [10] presented the heat treatment influences on the LCF and HCF properties of AZ91D and NZ30K alloys. They claimed that after the heat treatment, the AZ91D alloy indicated better LCF behavior than the HCF and this behavior was different for NZ30K alloy. Kuffova [11] compared the effect of annealing (T4) and ageing (T6) processes on the HCF properties of AZ91D alloy. They reported that the ageing process (T6) had a more significant effect on the fatigue lifetime and strength fatigue improvement and crack growth rate reduction than the annealing process (T4). Azadi et al. [12] characterized the temperature and time effects of solution treatment on the hardness of 713C superalloy. The optimum value of hardness was obtained in solution at 1200 °C for 1 hour. Their results illustrated that solution temperature was the most effective parameter on the hardness. Cavaliere and Marco [13] compared the effects of FSP and the heat treatment on the fatigue lifetime of AZ91 alloy. They found that the FSP increased the fatigue lifetime at high-stress levels much more than the heat treatment. Krupinski and Tanski [14] analyzed the sensitivity of tensile strength and hardness of AZ31, AZ61, and AZ91 to the heat treatment and different Al% concentrations. They reported that AZ91 alloy had higher tensile strength and hardness values, which included more Al% concentration, compared to the heat treatment. Bag and Zhou [15] compared the effect of solution and ageing processes on fatigue lifetime and tensile properties of AZ91 alloy. According to their results, the solution increased the fatigue lifetime, more than the ageing, by dividing the crack path into several smaller crack branches and reduction of stress intensity at the crack tip. Pokorny et al. [16] represented the hot tearing severity effect on the mechanical properties of AZ91D alloy. They found that the best hot tearing severity was obtained by changing the mold cast temperature from 140 °C to 380 °C. Vaidaya and Lewandowski [17] characterized the effects of adding SiCp and heat treatment on the fatigue strength of AZ91 alloy. They claimed that both addition and the heat treatment, contemporaneously, improved the fatigue limit from 120MPa to 150MPa, at 10^7 cycles. Xu et al. [18] evaluated the effect of adding 1% rare-earth (RE) element (1% MM) on the HCF regime of AZ91 alloy. They observed that the minority and majority of casting defects were in the free surface and core of the samples, respectively. That was the main reason for reducing fatigue lifetime.

In one research, Yang et al. [19] conducted the effect of adding 1% cerium (RE) on the HCF behavior of AZ91 alloy. They found that the fatigue limit in-

creased from 96MPa to 116MPa in 10^7 cycles, due to a significant decrease in grain size or increase in grain boundaries as a barrier against dislocation movement. In another research, Yang et al. [20] characterized the influence of adding 1% neodymium (RE) on the HCF properties of AZ91 alloy. Based on their results, the fatigue limit improved from 76MPa to 86MPa in 10^7 cycles. Mokhtarishirazabad et al. [21] studied the HCF behavior of AZ91 alloy, under the influence of adding 1% rare earth element. They reported that, although hardness did not increase a lot; however, the fatigue limit increased more than 40% at 10^6 cycles.

According to the above introduction, it could be claimed that the research on the sensitivity analysis of the HCF lifetime for AZ91 alloy is still rare. Moreover, as another novelty, the influences of the RE element addition and the heat treatment were obtained besides the stress effects. Therefore, HCF testing was done on standard samples under stress-controlled cyclic loading and then, the parameters of the stress level, the RE element, and the heat treatment were analyzed by the regression method.

2. Materials and Tests

2.1. Material Type

In this research, elements such as magnesium, aluminum, and commercial pure zinc with a purity of more than 99.9% were used to produce AZ91 alloy. Manganese (Mn) in mischmetal mode was added. The alloy (in a typical crucible made of carbon steel) melted in a resistance furnace, under the atmosphere ($\text{CO}_2 + \text{HFC-134a}$) at 750°C. The chemical composition of the produced alloy is specified by inductively coupled plasma. Rare-earth (RE) elements of Cerium-rich type with a ratio of Cerium to Lanthanum 2.9, were added and the added amounts of Neodymium (Nd), Praseodymium (Pr), Lanthanum (La), and Cerium (Ce) were 2%, 7%, 26%, and 67%, respectively. The melt was kept at 750°C for half an hour and 300°C for preheating in the bottom-filled steel die. Table 1 shows the amount of chemical composition of the alloys.

Table 1
The chemical combinations (in wt.%) of used alloys.

Alloy	Al	Zn	Mn	Fe	Ce	La	Mg
AZ91	9.43	0.93	0.19	-	-	-	Balance
AZE911	8.84	0.81	0.14	0.09	0.64	0.33	Balance

2.2. Heat Treatments

The solution was performed at a temperature of 415°C for 5 hours. The AZ91 alloy was aged at the temperatures of 215°C and 3 hours and also AZE911 alloy was aged at the temperature of 215°C for 5 hours (Fig. 1).

The quenching was in the air. All stages of the heat treatment (solution and ageing) were performed in a tube furnace under the controlled atmosphere of CO₂ gas.

2.3. High-cycle Fatigue Testing

After casting, the standard samples of fatigue testing were machined based on the ISO-1143 standard. The applied loading or stress levels of AZ91, AZE911, AZ91-H6, and AZE911-H6 alloys are shown in Table 2 by a rotary fatigue tester (SFT-600), depicted in Fig. 2. The stress ratio and loading frequency are -1 and 100 Hz, respectively. The geometry of the fatigue testing specimen could be seen in Fig. 2. The samples which did not fail or break at 10⁶ cycles in each stress level are called “Run-Out”.

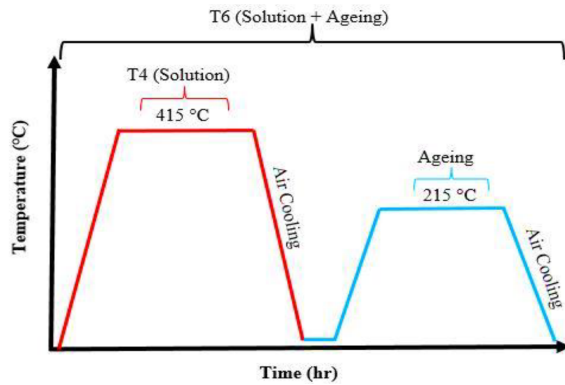


Fig. 1. The cycle of T4 and T6 Heat treatments.

Each high-cycle fatigue (HCF) testing was repeated only once at the stress level leading to fatigue limit and at other low- and high-stress levels, at least 3 times and

at most 5 times. This value was based on the scatter-band that was exhibited through testing. Whether if the scatter-band was narrow, a lower number of experiments was done. In some other cases, the samples were broken very quickly and in less than 5,000 cycles, which have been removed due to the large number and the large size of the casting defects such as porosities, inclusions, and voids. The tests were done 11, 17, 11, and 12 times in different stress levels, for AZ91, AZ91-HT, AZE911, and AZE911-HT alloys, respectively.

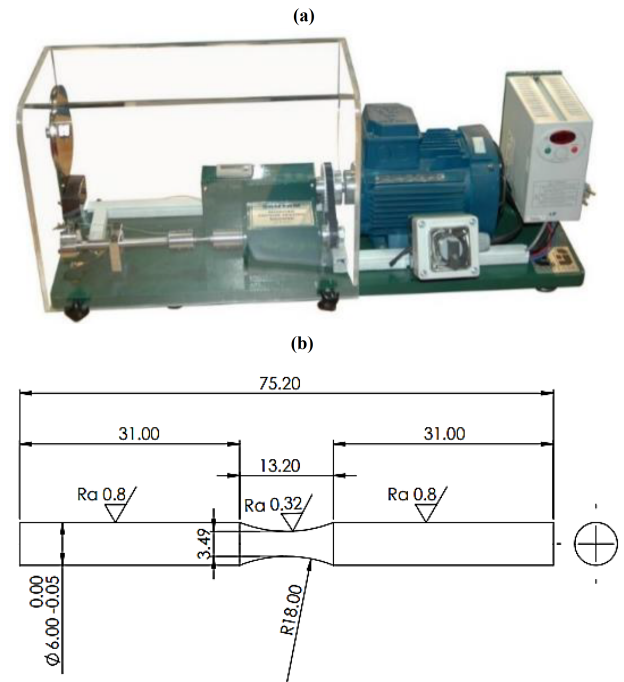


Fig. 2. a) Fatigue testing device and b) The geometry of fatigue samples.

Table 2
The condition of loading (in MPa) on the materials.

Alloy	Applied stress levels (MPa)	Heat treatment	Rare-earth addition	Test repeatability
AZ91	64	No	No	1
AZ91	75	No	No	2
AZ91	85	No	No	3
AZ91	95	No	No	3
AZ91	105	No	No	2
AZ91	105	No	Yes	1
AZ91	115	No	Yes	3
AZ91	115	Yes	No	4
AZ91	125	No	Yes	3
AZ91	125	Yes	No	4
AZ91	135	No	Yes	2
AZ91	135	Yes	No	4
AZ91	145	No	Yes	2
AZ91	145	Yes	No	5
AZ91	155	Yes	Yes	2
AZ91	165	Yes	Yes	3
AZ91	175	Yes	Yes	4
AZ91	185	Yes	Yes	3

Table 2 shows the number and conditions of fatigue testing, before performing the regression analysis on experimental data. In total, 11, 17, 11, and 12 tests were performed for AZ91, AZ91-T6, AZE911, and AZE911-T6 alloys, respectively.

2.4. Sensitivity Analysis

For creating a correct perception and optimizing the effect of different parameters on a response, the design of the experiment (DOE) was utilized, which includes several methods and several sections. In addition to qualitative evaluation, regression analysis was used for quantitative results, which is a statistical proceeding for finding the relations between parameters [22]. Regression analysis helps to see how the value of the dependent parameter changes as each of the changes of the independent parameters and the other independent parameters do not change. In quantitative analysis, the value of standard deviation indicates, on average, how far the data are from the mean [23].

Sensitivity analysis was performed in the DESIGN EXPERT software. Input data were the stress, the heat treatment, and rare-earth element (1% RE) addition. Output data were the normal and logarithmic fatigue lifetime. Then, these results were found by statistical process, like the regression method, to find the most effective parameters. Controlling factors in the sensitivity analysis consist of the coefficient of determination (R^2), F-Value, and the P-Value. These values were utilized to check the quality of the regression analysis [23]. The effectiveness of inputs could be determined by the F-Value, comparing df_0 to $df_{n,n-1,N-n}$. The risk value is 0.05, based on 95% of confidence level. Then, $n - 1$ and $N - n$ show the degree of freedom for the action and the error. The F-Value is calculated by Equation (1):

$$df_0 = MS_{\text{action}}/MS_{\text{error}} \quad (1)$$

where $df_{n,n-1,N-n}$ is found in ANOVA tables. The P-Value must be less than 0.05. When the P-Value is higher than 0.05, the factor is not effective (not significant). For determining the quality of fitting data to the applied model, the R^2 value is used. For the unity value of R^2 , the curve-fitting is accurate for all data [23].

For outputs, the fatigue lifetime and the objective function in our study were determined by two models. The first one is based on Equation (2):

$$f_{\text{objective}} = D_0 + D_1P_1 + D_2P_2 + D_3P_1P_2 + D_4(P_1)^2 + \dots \quad (2)$$

where D_i and P_i are constants and inputs, respectively. The first exponent (P_1) and the second exponent ($(P_1)^2$), the interaction of parameters (P_1P_2),

were used. And the second model is written as Equation (3):

$$\log(f_{\text{objective}}) = D_0 + D_1 \log(P_1) + D_2 \log(P_2) + D_3 \log(P_1) \log(P_2) + \dots \quad (3)$$

Table 3 demonstrates the signs and descriptions of the performed processes on the alloys.

3. Results and Discussions

Table 4 shows the changes between stress levels and fatigue lifetime amplitude (cycles) to fracture or failure for the AZ91 alloy. In one stress level, HCF lifetime is dependent on the size (small or big), number (a few or a lot), distribution (concentration or far from each other), and different locations of defects (in the surface or core of specimen) [24]. As observed in Table 4, the fatigue limit of AZ91 alloy is at 65MPa and 10^6 cycles. In addition, when stress level increased from 65MPa to 105MPa, the fatigue lifetime decreased from 10^6 cycles to 7.3×10^4 cycles.

Table 5 illustrates the stress levels and fatigue lifetime amplitude of AZ91 alloy, after 1% RE element addition (AZE911). The most influential effects of the RE element addition are as follows:

1. The RE element addition has a direct effect on reducing the size, amount, or number, increasing the distribution of cast defects.
2. The fatigue strength before RE element addition was 65MPa (Run-Out) and, after that, increased to 105MPa, both at 10^6 cycles (Run-Out).
3. Each stress level improved by more than 30%. For example, the stress level reached from 85MPa to 125MPa at 3.4×10^4 cycles (47% enhancement), 85MPa to 135MPa at 10^5 cycles (59% enhancement), and 95MPa to 125MPa at 3.8×10^5 cycles (31% enhancement).

The RE element addition affects the size and distribution of the cast defects and Beta precipitations, the most influential factors on the HCF properties of AZ91D alloy. In general, three separated steps of fatigue damage in the HCF loading regime. The first step is crack incubation, which is incubated approximately merely at the cast defects or large porosities inside the samples. The second step is small cracks that grow along the poor grain boundaries and arm dendrites, and finally, the third step is long cracks grow in a trans-granular mode [11–15]. Samples with a lot of cast defects during limited getting exposed to cyclic loading, but those with a few cast defects tolerate more cycles [32, 38]. The RE element addition by decreasing the size and number of cast defects, decreasing grains size of Alpha and Beta phases, and

finally hardening or refinement of grains, could have been able to greatly reduce the negative effects of these steps on the fatigue lifetime, for each stress level [18–21]. Xu et al. [18] and Yang et al. [19, 20] reported the fatigue lifetime changes under the influence of the RE element addition. After the addition of 1% rich in Cerium mischmetal [18], 1% Cerium [19] and 1% neodymium [20], the stress levels increased from 50-62MPa to 70-110MPa [18], 92-104MPa to 110-120MPa [19], 50-62MPa to 76-92MPa [20], all at fatigue lifetime range of $10^5 - 10^7$ cycles. It means that, although they investigated the HCF lifetime of AZ91 alloy after the addition of rare elements at higher stress levels, the fatigue lifetime range was not reduced and remained

constant ($10^4 - 10^7$ cycles). It means that the destructive effect of higher stress levels on casting defects, in terms of forming sooner cracks and failure, has been controlled or neutralized by the addition of rare elements, and the specimens have been able to lifetime at higher stress levels, at the same range [6, 21].

Yang et al. [19, 20] and Xu et al. [18] agreed with each other that, after RE element additions, there was a good improvement in fatigue limit and a large fatigue lifetime amplitude ($10^5 - 10^7$ cycles), but at low-stress levels. In other words, if the stress levels were chosen more than 120MPa, the fatigue lifetime amplitude should be decreased from $10^5 - 10^7$ cycles to $10^4 - 10^6$ cycles.

Table 3

Abbreviations for fatigue test samples in this research.

Number	Abbreviations	Explanations
1	AZ91-H0	Magnesium-aluminum-zinc alloy
2	AZE911-H0	Magnesium-aluminum-zinc alloy reinforced with 1% rare-earth addition
3	AZ91-H6	Magnesium-aluminum-zinc alloy the heat treatment
4	AZE911-H6	Magnesium-aluminum-zinc alloy reinforced with 1% rare-earth addition the heat treatment

Table 4

The loading or applied stress levels of AZ91 alloy.

Number Sample	Stress amplitude σ_a (MPa)	Fatigue lifetime N_f (cycle)	Average fatigue lifetime N_f (cycle)	Standard deviation of fatigue lifetime N_f (cycle)	Descriptions
AZ91-1	64.6	1,030,000	1,030,000	-	Run-out, no failure
AZ91-2	74.5	265,440	383,093	117,653	OK
AZ91-3	74.5	500,745			OK
AZ91-4	84.7	34,296	244,040	242,625	OK
AZ91-5	84.7	113,740			OK
AZ91-6	84.7	584,085			OK
AZ91-7	94.6	382,122	153,331	163,334	OK
AZ91-8	94.6	11,400			OK
AZ91-9	94.6	66,471			OK
AZ91-10	104.5	30,136	51,710	21,574	OK
AZ91-11	104.5	73,283			OK

Table 5

The loading or applied stress levels of AZE911 alloy.

Number Sample	Stress amplitude σ_a (MPa)	Fatigue lifetime N_f (cycle)	Average fatigue lifetime N_f (cycle)	Standard deviation of fatigue lifetime N_f (cycle)	Descriptions
AZE911-1	104.6	1,020,000	1,020,000	-	Run-out, no failure
AZE911-2	114.5	38,258	25,5353	293,454	OK
AZE911-3	114.5	57,592			OK
AZE911-4	114.5	670,210	150,239	166,896	OK
AZE911-5	124.7	26,857			OK
AZE911-6	124.7	37,677			OK
AZE911-7	124.7	386,183	117,291	20,468	OK
AZE911-8	134.6	96,823			OK
AZE911-9	134.6	137,759			OK
AZE911-10	144.4	25,325	55,253	29,928	OK
AZE911-11	144.4	85,181			OK

Table 6
The loading or applied stress levels of AZ91-H6 alloy.

Number Sample	Stress amplitude σ_a (MPa)	Fatigue lifetime N_f (cycle)	Average fatigue lifetime N_f (cycle)	Standard deviation of fatigue lifetime N_f (cycle)	Descriptions
AZ91-H6-1	114.5	132,000			OK
AZ91-H6-2	114.5	2,004,000			Run-out, no failure
AZ91-H6-3	114.5	2,124,000	1,070,000	994,323	Run-out, no failure
AZ91-H6-4	114.5	25,200			OK
AZ91-H6-5	124.5	97,600	144,125	143,290	OK
AZ91-H6-6	124.5	88,400			OK
AZ91-H6-7	124.5	384,500			OK
AZ91-H6-8	124.5	6,000			OK
AZ91-H6-9	134.6	52,500			OK
AZ91-H6-10	134.6	94,400			OK
AZ91-H6-11	134.6	29,500	50,100	27,721	OK
AZ91-H6-12	134.6	24,000			OK
AZ91-H6-13	144.7	10,200			OK
AZ91-H6-14	144.7	71,000			OK
AZ91-H6-15	144.7	19,300	22,060	25,031	OK
AZ91-H6-16	144.7	4,400			OK
AZ91-H6-17	144.7	5,400			OK

Xu and Han [25] claimed that after 2% Yttrium addition to Mg-6wt%Zn-0.8wt%Zr alloy, for all S-N curves, there was a plateau in the range of $5 \times 10^6 - 10^8$ cycles, and then the fatigue limit step by step reduces between 10^8 and 10^9 cycles. Therefore, just a fatigue limit corresponding to 10^9 cycles could be appointed. The fatigue limit of the alloy with 2% Yttrium addition was 105MPa. Furthermore, fatigue crack initiated at the surface of the samples in the range of $10^6 - 10^9$ cycles.

In Table 6, the changes in stress levels and fatigue lifetime amplitude of AZ91 alloy, after heat treatment (AZ91-H6), are presented. The most significant effects of heat treatment are as follows:

1. The heat treatment does not affect the cast defects.
2. The heat treatment has the same product (or impact rate) on the stress level improvement, as the RE element (comparing Tables 5 and 6).
3. The fatigue strength before heat treatment was 65MPa (Run-Out) and, after that, increased to 115MPa, both at 10^6 cycles (Run-Out).

The heat treatment had the same effect on the fatigue limit of AZ91 alloy, as much as adding the RE element in each stress level, but increased the fatigue lifetime amplitude more than adding RE. Heat treatment compared to the RE element addition has not been able to control the effects of cast defects (especially at high-stress levels), still, it does not mean decreasing fatigue lifetime amplitude. Heat treatment significantly reduced grain size and increased the number of

grains, grain boundaries, and micro-hardness. On one hand, decreasing the grain size and also increasing the micro-hardness of the phases are the most substantial and difficult barriers against crack growth rate and dislocation movement during plastic deformation, which resulted in improved fatigue lifetime at higher stress levels [13, 15, 26–29]. On another hand, the increasing number of grains after the heat treatment, caused the higher applied stresses to be distributed among more grains and more hardened grains. Therefore, the effect of stress intensity is reduced, and finally, the samples were able to tolerate the higher stress levels and work until the expected fatigue lifetime [11, 32–36].

Li et al. [28] reported the changes in the HCF behavior of NZ30K-T6 and AZ91-T6 alloys, under the influences of the heat treatment and test temperatures (25°C and 150°C). They concluded that the fatigue limit of NZ30K-T6 and AZ91-T6 alloys, was 90MPa and 65MPa, respectively, at 25°C and 10^7 cycles. They presented a model using the sizes of the cast defects for predicting the fatigue lifetime of the samples containing oxide films. Because these oxide films decrease the fatigue lifetime, especially at 150°C . The fatigue fracture performance of both alloys casts is characterized by the Weibull modulus and the feature fatigue lifetime.

Yang et al. [29] investigated the effects of T4 heat treatment (solution) on the HCF properties of the AZ91D alloy. Based on their results, the fatigue limit increased from 55MPa to 72MPa, after T4 heat treatment at 415°C for 16 hours, at 10^7 cycles. In similar research, the fatigue limit was reported as 60MPa (at 10^7 cycles) by Nemcova et al. [30]. They also expected

that ageing and artificial ageing treatments could be more effective than the solution on the HCF properties [10–14]. As an example, Kuffova [11] claimed that the fatigue limit increased between 120MPa and 150MPa after T6 heat treatment (ageing after solution) and also increased between 150MPa–200MPa, after T4 heat treatment (solution), both at $10^4 - 10^6$ cycles. Moreover, the effectiveness of each of these processes (T4 and T6) was different. Cavaliere and Marco [13] with Bag and Zhou [15] both jointly concluded that T6 heat treatment had no significant effect on fatigue lifetime improvement and the effect of T4 was significantly greater than T6 on fatigue lifetime of AZ91 alloy.

Table 4 shows the changes in stress levels and fatigue lifetime amplitude of AZ91 alloy after the simultaneous effect of adding 1% RE element and performing heat treatment (AZE911-H6). The most significant impacts of 1% RE element addition and heat treatment (together) are as follows:

1. The destructive effects of cast defects decreased dramatically on fatigue lifetime, especially at higher stress levels.
2. There was no fatigue limit (Run-Out) for AZE911-H6 alloy because the applied stress levels were very high (155, 165, 17, and 185MPa). These applied stress levels are usually used for HCF loading of some aluminum alloys, such as A319, A356, and A380, not a magnesium alloy like AZ91.
3. Each stress level improved by more than 50%. For example, at 3.8×10^5 cycles, the stress level reached from 95MPa to 155MPa at 3.4×10^4 cycles (63% enhancing) and from 95MPa to 165MPa at 6.6×10^4 cycles (73% enhancing).

AZ91 alloy, after heat treatment and the RE element addition, was able to tolerate higher stress levels

at the same range of fatigue lifetime ($10^4 - 10^6$ cycles). The effect of heat treatment on the fatigue lifetime in some stress levels was more than the RE elements addition. For example, at 115 and 125MPa, adding RE elements causes the AZ91 samples to work up to 0.8 million and 3.7×10^4 cycles, respectively, and heat treatment causes the samples at the same stress levels (115 and 125MPa) to work up close to 2.5 million and 9.7×10^5 cycles, respectively. The refining of the grains could be gained by small RE element additions to alloy, although the discontinuously precipitated Beta phases still existed on grain boundaries.

Mokhtarishirazabad et al. [31] discussed the sensitivity of the low-cycle fatigue (LCF) of the AZE911 Mg alloy to the parameters of stress, test temperatures, and different heat treatments. They reported that at low temperatures, the lifetime in the LCF regime, improved by the solution process but reduced by the ageing process (a little). For high temperatures, this demeanor is reversed, and the heat treatment significantly affects the LCF lifetime. The LCF lifetime at high temperature of the AZE911 Mg alloy (in heat- and un-heat-treated conditions) was much more than the low-temperature. This influence was more substantial in the aged alloy.

The obtained results, including the trend behavior, are put in Tables 8 and 9 as a general conclusion. Tables 8 and 9 depict the influences of inputs on outputs of fatigue test, including general behavioral trends.

Fig. 3a demonstrates the sensitivity of fatigue lifetime to stress, the RE element addition, or the material type on the heat-treated and none-heat-treated AZ91 and AZE911 alloys at different stress levels. According to this figure, the stress level range of AZ91 alloy after adding RE increased from 65–105MPa to 105–145MPa in $10^4 - 10^6$ cycles, and the stress level range of AZ91-H6 alloy increased from 115–145MPa to 155–185MPa at the same cycles. It means that the RE element addition did not affect the lifetime amplitude.

Table 7

The loading or applied stress levels of AZE911-H6 alloy.

Number Sample	Stress amplitude σ_a (MPa)	Fatigue lifetime N_f (cycle)	Average fatigue lifetime N_f (cycle)	Standard deviation of fatigue lifetime N_f (cycle)	Descriptions
AZE911-H6-1	155.3	354,000	495,550	141,550	OK
AZE911-H6-2	155.3	637,100			OK
AZE911-H6-3	165.5	48,000	47,033	16,793	OK
AZE911-H6-4	165.5	67,100			OK
AZE911-H6-5	165.5	26,000			OK
AZE911-H6-6	176.0	8,000	31,125	24,322	OK
AZE911-H6-7	176.0	60,000			OK
AZE911-H6-8	176.0	50,400			OK
AZE911-H6-9	176.0	6,100			OK
AZE911-H6-10	185.7	33,600	23,600	8,165	OK
AZE911-H6-11	185.7	13,600			OK
AZE911-H6-12	185.7	23,600			OK

Table 8

Inputs include stress, material type, and heat treatment in the DESIGN EXPERT software.

Factor	Name	Type	Min.	Max.	Low	High	Mean	Std. Dev.
A	Stress (MPa)	Numeric	64.60	185.70	64.60	185.70	129.96	31.18
B	Material type	Categoric	AZ91	AZE911	-	-	Levels:	2.00
C	Heat treatment	Categoric	H0	H6	-	-	Levels:	2.00

Table 9

Outputs include normal and logarithmic fatigue lifetime in the DESIGN EXPERT software.

Response	Name	Minimum	Maximum	Mean	Std. Dev.	Ratio
R1	Lifetime (cycle)	4400	2004000	236200	436100	455.45
R2	Log (Lifetime)	3.64345	6.3019	4.85	0.6788	1.73

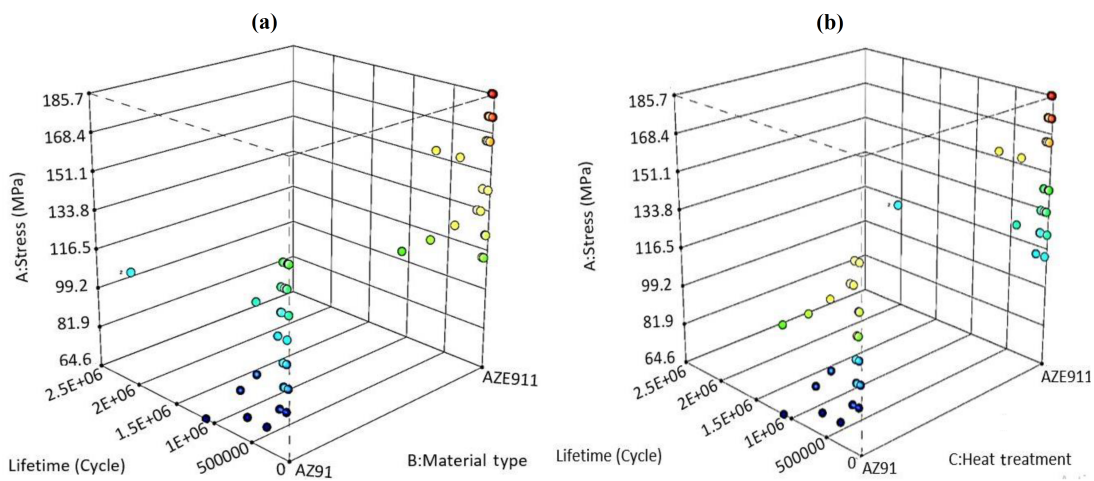


Fig. 3. The effects of the factors for a) The material type and b) The heat treatment in the DESIGN EXPERT software

On the contrary, Fig. 3b shows the effect of heat treatment on the fatigue lifetime of AZ91 and AZE91 alloys and reports that the AZ91 alloy stress level range after heat treatment has increased from 65–105MPa at $10^4 - 10^6$ cycles to 115–155MPa at $10^3 - 2.5 \times 10^6$ cycles. In other words, a 150% improvement in the fatigue lifetime, caused an incredible increase in fatigue lifetime amplitude. Finally, the AZE911 alloy stress level range increased from 105–145MPa at $10^4 - 10^6$ cycles to 155–185MPa at $10^4 - 7.6 \times 10^5$ cycles. Thus, its fatigue lifetime amplitude had a small decrease, which goes back to the interaction effects of stress and heat treatment. That means although the fatigue lifetime amplitude of AZE91 alloy had to be increased by the heat treatment, still, because of applying very high-stress levels (155, 165, 175, and 185MPa), this positive effect of the heat treatment was significantly controlled or reduced for improving the fatigue lifetime amplitude. It should be mentioned that these applied stress levels are as much as stress levels of some known cylinder head aluminum alloys, like A319, A356, and A380 in the HCF regime. The stress levels and then heat treatment are the most significant factors for improving the fatigue lifetime amplitude, respectively.

Afsari Golshan et al. [32] studied the sensitivity analysis of creep lifetime of AlSi12CuNiMg alloy under the effects of applied loading (stress levels), heat treatment, and test temperature. They concluded that heat treatment as the most influential parameter improved the creep lifetime amplitude by 63% and reduced the strain rate effects. Azadi and Aroo [33] studied the sensitivity of the fatigue lifetime of aluminum alloys to the parameters of the heat treatment, the addition of nano-particles, the applied stress, and the test environment corrosion rate. They claimed that heat treatment was the most influential parameter due to improving the fatigue lifetime more than ten times. Fatigue and fatigue-corrosion lifetimes of the aluminum alloy, refined with the heat treatment and nano-particles, enhanced by 114 and 128%, respectively, under high-stress loading, compared to the base aluminum alloy. Aroo et al. [34] evaluated the effects of nano clay addition, heat treating, and acid percentage on the corrosion resistance time of piston aluminum alloy. According to their sensitivity analysis results, nano clay addition was the most effective factor for improving corrosion resistance time, but it was reversed for acid percentage and specially heat treating.

To have an acceptable regression model, a P-Value must be less than 0.05. After that, the R^2 Value should be as high as possible. The highest value is unity for the accurate fitting of data by the model. Then, each factor in inputs must be controlled, whether it is impressive or not. As mentioned, for an effective factor, the P-Value must be less than 0.05. Then due to the importance of all factors in comparison with each other, the F-Value was utilized. A higher F-Value shows a higher effect of the factors on the inputs [22, 23].

Tables 10 and 11 include the obtained results of the fatigue test by distinct inputs in the DESIGN EXPERT software. Inputs were the stress levels (loading), a continuous factor, and the heat treatment, as a separated factor. Then, these tables are for the objectives of the fatigue lifetime. Furthermore, outputs were provided into different measures to find the better model in the regression analysis. Tables 10 and 11 indicate the F-Value, P-Value, the R^2 Value, and effects rate of elements, in normal and logarithmic states, respectively. Then, according to these values, the better model has been chosen [22, 23].

The ANOVA table (Tables 10 and 11), based on the reduced cubic model, provides values of F-Value, P-Value, degree of freedom for the factors of stress, heat treatment, and the RE element addition on the fatigue lifetime in both normal and logarithmic states. On the one hand, the stress factor has the lowest P-Value (0.0001 in normal and logarithmic states) and the P-Value of the RE element addition (0.0190) and heat treatment (0.0024) are much more than 0.0001. On the other hand, the stress factor has the highest F-Value (28.75) and the P-Value of the RE element addition and heat treatment are 5.96 and 10.44, respectively. As a result, stress has a much greater effect on the fatigue lifetime compared to other factors. In addition, Table 10 indicates the degree of positive or negative impacts of each factor separately or together. Since the F-Value for the stress is much more than its interaction with other factors. The F-Value of interaction between the stress with the RE element addition (6.25) and heat treatment (8.76) is less than the F-Value of stress (28.75). In other words, it looked that the stress had more influences on outputs than its interaction with the RE element addition (the material type) and the heat treatment. Comparing the F-Value and P-Value of the RE element addition (the material type) and the heat treatment express that the heat treatment has more F-Value and less P-Value than the RE element addition (the material type). Therefore, the heat treatment is more effective than the RE element addition (the material type) on the fatigue lifetime. Table 11 illustrates all mentioned points just in a logarithmic state.

Figs. 4a and 4b show the interaction plots in logarithmic and normal states, respectively. These plots depict how the dependency of the relationship between a definite factor, as the RE element addition (the ma-

terial type), and continuous response, as the fatigue lifetime to the value of the second definite factor, as heat treatment. These plots demonstrate goals for the levels of the material type or the RE element addition factor on the x-axis and a discrete line for each level of heat treatment factor. The actual factor (A) for both logarithmic and normal interaction plots is 125.15. In this case, for the none heat-treated alloys, the fatigue lifetime amplitude did not change by the addition of RE, and for the heat-treated alloys, this behavior was reversed. From another point of view, there was an interaction between the RE element addition and the heat treatment for the fatigue lifetime, in Figs. 4a and 4b. Therefore, the lines were cross or nonparallel and meant an interaction occurred.

In one study, Azadi et al. [35] reported that the yield strength, the young modulus, and the elongation were sensitive to the interaction or the multiply of the SiO_2 nano-particle addition and the loading rate. The loading rate had just one impressive effect on the young modulus and the elongation. Furthermore, the yield strength was sensitive to both factors, the SiO_2 nano-particle addition, and the loading rate. In another paper, Azadi et al. [36] studied the test temperature and nano-particle addition effects on the mechanical properties of the piston AlSi alloy. They indicated that the test temperature at 250°C and nano-particle addition increased the tensile and yield strengths, elastic module, and elongation, separately, but the interaction between these two factors showed a negative or reverse effect on the mentioned properties. Safarloo et al. [37] used a regression model for the temperature and time ageing in heat treatment on the hardness of Inconel-713C superalloy. They concluded that the optimum hardness value was obtained after ageing at 890°C for 8 hours. Based on their DOE results, the highest hardness value is predicted in two ageing at 896.1°C for 8 hours and 895.3°C for 16 hours, with and without interaction between ageing time and temperature, respectively. In addition, the effect of ageing time was more than the ageing temperature.

Enhancing the fatigue lifetime of Mg alloys by the reinforcement was also studied by Azadi et al. [35, 36] and Azadi and Aroo [33], which would be able as a sign of agreement with found results in this study. The reason for this enhancement was because of the phases and especially grain changes in the microstructure.

Based on obtained results in Fig. 4, the effect of each parameter, either simultaneous or together influence of heat-treating and the RE element, in terms of improving the fatigue lifetime and the fatigue limit of the AZ91 magnesium alloy was greater than the separate effect of the heat treatment or the RE element addition. Moreover, increasing the stress level, which reduced the fatigue lifetime, had a stronger impact on the HCF lifetime of the material, than other parameters.

Table 10

Response results of data analysis in the DESIGN EXPERT software for the normal fatigue lifetime.

Source	Sum of squares	Df	Mean square	F-value	P-value	Status
Model	4.497E+12	8	5.621E+11	4.71	0.0004	Significant
A-stress (MPa)	3.431E+12	1	3.431E+12	28.75	< 0.0001	Significant
B-material type	7.110E+11	1	7.110E+11	5.96	0.0190	Significant
C-heat treatment	1.246E+12	1	1.246E+12	10.44	0.0024	Significant
AB	7.456E+11	1	7.456E+11	6.25	0.0164	Significant
AC	1.045E+12	1	1.045E+12	8.76	0.0050	Significant
BC	7.009E+11	1	7.009E+11	5.87	0.0198	Significant
A ²	1.017E+12	1	1.017E+12	8.52	0.0056	Significant
ABC	6.430E+10	1	6.430E+10	0.5387	0.4670	not significant
Residual	5.013E+12	42	1.194E+11	-	-	-
Lack of fit	5.387E+11	9	5.985E+10	0.4415	0.9023	not significant
Pure error	4.474E+12	33	1.356E+11	-	-	-

Table 11

Response results of data analysis in the DESIGN EXPERT software for the logarithmic fatigue lifetime.

Source	Sum of squares	Df	Mean square	F-value	P-value	Status
Model	11.69	8	1.46	5.41	0.0001	Significant
A-stress (MPa)	8.18	1	8.18	30.25	< 0.0001	Significant
B-material type	3.15	1	3.15	11.67	0.0014	Significant
C-heat treatment	2.98	1	2.98	11.04	0.0019	Significant
AB	0.5371	1	0.5371	1.99	0.1660	not significant
AC	0.9598	1	0.9598	3.55	0.0664	not significant
BC	0.7605	1	0.7605	2.81	0.1009	not significant
A ²	0.7281	1	0.7281	2.69	0.1082	not significant
ABC	0.0425	1	0.0425	0.1573	0.6937	not significant
Residual	11.35	42	0.2703	-	-	-
Lack of fit	0.9722	9	0.1080	0.3435	0.9532	not significant
Pure error	10.38	33	0.3145	-	-	-

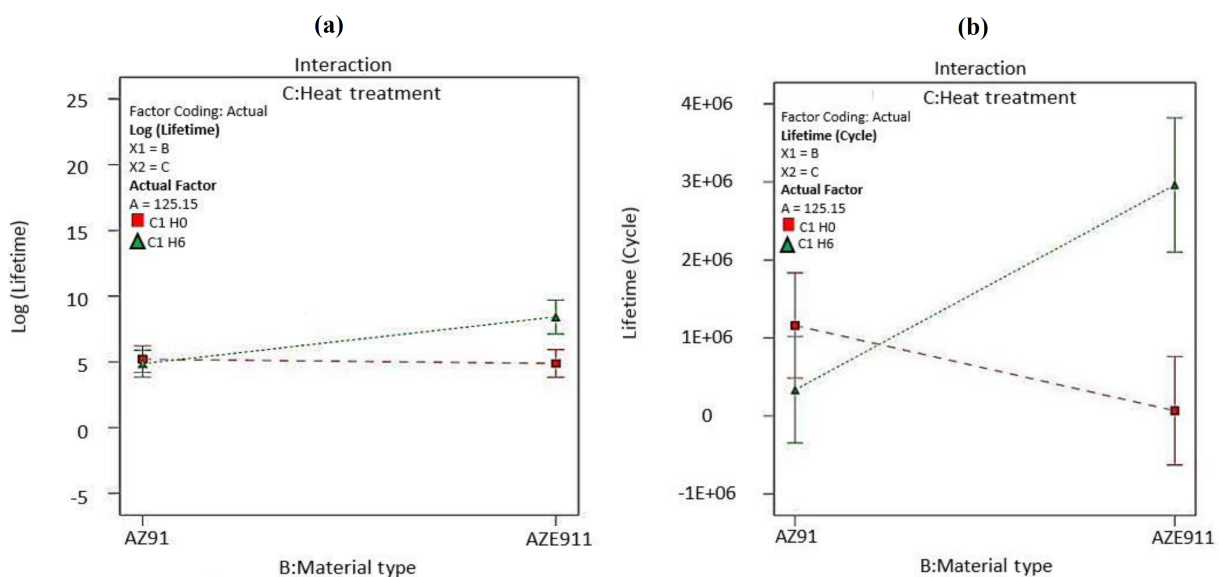


Fig. 4. The results of interaction plots for a) Logarithmic and b) Normal fatigue lifetimes.

Figs. 5a and 5b display the predicted versus actual plot of logarithmic and normal fatigue lifetime, respectively. Moreover, Figs. 6c and 6d illustrate the residual plots of logarithmic and normal fatigue lifetime, respectively. The choice model has more than one explanatory parameter, and it is not practical to represent more in a chart like that. Thus, instead, it has plotted the predicted values versus the observed values for these same data sets of fatigue lifetime. For an exact fitting, the observed and predicted fatigue lifetime values should be close to each other or they should be close to the fitted line with narrow confidence bands. In

other words, the fatigue lifetime ranges or amplitudes after the RE element addition and heat treatment are in $10^4 - 10^6$ cycles and $10^3 - 2.5 \times 10^6$ cycles, respectively, which are too close to each other. Therefore, the majority of fatigue lifetime values are near or on the fitted line, which is shown in the green cadre (Fig. 5a). In addition, the fatigue lifetime values of more than 10^6 cycles and less than 10^4 cycles are far from each other and also the fitted line, which is depicted in the red cadre (Fig. 5a). This condition is the same for logarithmic and normal fatigue lifetime in the normal plot of residuals.

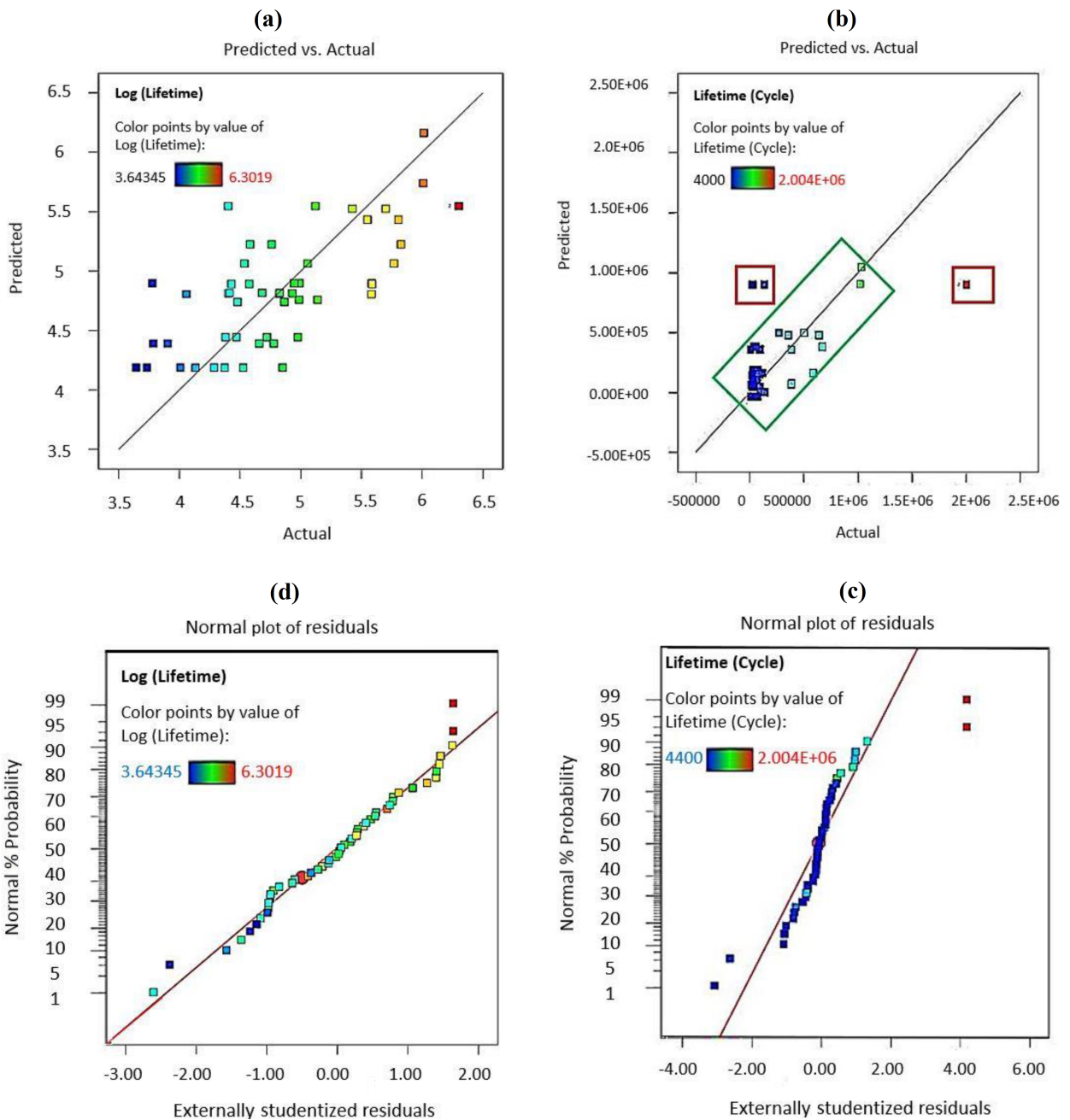


Fig. 5. The plot of the predicted versus actual data for a) Logarithmic and b) Normal fatigue lifetimes, and the plot of the probability for c) Logarithmic and d) Normal fatigue lifetimes.

Table 12

The formulation for regression analysis.

Outputs	Lifetime (cycle)	P-values	Log (lifetime)	P-values
Intercept	1.13062E+06	-	5.84294	-
A	-1.5827E+06	< 0.0001	-2.44297	< 0.0001
B	383414	0.0190	0.807417	0.0014
C	517662	0.0024	0.800849	0.0019
AB	-2.47631E+06	0.0164	-2.10174	0.1660
AC	-3.18742E+06	0.0050	-3.0543	0.0664
BC	929964	0.0198	0.968677	0.1009
A ²	4.15734E+06	0.0056	3.51851	0.1082
ABC	188923	0.4670	-0.15359	0.6937

The normal probability plot of the residuals is almost linear, supporting the state that the error terms are normally distributed. The fitted lines in Figs. 5c and 5d indicate extremely exceptionally and accurate residual plots for both logarithmic and normal fatigue lifetime, respectively. Weibull distributions could illustrate the distributions of fatigue lifetime at the consistent stress amplitude. As an agreement and similar results, Ishihara et al. [38] worked on the Weibull distributions of the size of cast defects on the HCF lifetime of the AZ91 alloy using predicted versus actual plots. Based on their results, defects larger than 50 μm^2 were just measured and plotted in the Weibull distributions. The ranges for allocations of the higher stress levels (100 and 120MPa) are approximately similar to each other. Therefore, the scatter in the fatigue lifetime distribution becomes smaller at the higher stress level than those at the lower stress levels (80MPa). The parameters of Weibull distributions demonstrate the distributions of the sizes and densities for the cast defects in the whole cross-section of the samples.

As another agreement, Mayer et al. [39] specified the maximum damage porosity in all samples and used the cast defect size for correlation with the endurance limit and fatigue lifetime. They presented distributions of cast defect areas in a logarithmic-normal probability plot. The ordinate shows the probability of cast defect size is bigger than the size indicated on the abscissa. The precision likelihood of cast defect size of the Mg alloys is almost linear, indicating the presence of a logarithmic-normal distribution. Anyway, it is less exact to describe AlSi9Cu3 alloy as a logarithmic-normal distribution, but to compare the Mg and Al alloys, both of them appraised based on the same distribution.

In statistics, the likelihood-ratio test evaluates the advantage of fit of two statistical competition models, according to the ratio of their likelihoods, obviously one obtained by maximization over the all factor space and another obtained after imposing some limitations. If the experimental or observed data supported the restriction (the null hypothesis), the two likelihoods cannot vary by more than sampling error. Thus,

the likelihood-ratio test examines whether this ratio is entirely different from one, or equivalently whether its natural logarithm is completely different from zero [40]. The Log-Likelihood ratio (χ^2) values of the stress, the RE element addition, and the heat treatment were 1.072E+07, 2.380E+06, and 2.675E+06, respectively for the P-value of less than 0.0001 for all factors. Table 13 depicts the most influential factor with the highest value of Log-Likelihood ratio (χ^2), which is equal to 1.072E+07. According to the explanations of the Likelihood table analysis, the used link is logarithmic and the inverse link is an exponential distribution. All P-values are less than 0.0001 and χ^2 shows the Log-Likelihood ratio when the response is the lifetime (in cycles). It should be noted that the Poisson regression is type III, and finally, ML stands for Likelihood analysis.

Table 13

The Likelihood analysis results.

Source	Df	χ^2	P-value
Model	8	1.559E+07	< 0.0001
A-stress (MPa)	1	1.072E+07	< 0.0001
B-material type	1	2.380E+06	< 0.0001
C-heat treatment	1	2.675E+06	< 0.0001
AB	1	2.430E+05	< 0.0001
AC	1	6.308E+05	< 0.0001
BC	1	5.236E+05	< 0.0001
A ²	1	2.937E+05	< 0.0001
ABC	1	22391.90	< 0.0001

Fig. 6 shows the logarithmic values of the lifetime and the stress in the S-N diagram for AZ91 alloy, with and without heat treatment and also with and without RE elements.

Fig. 7a, 7b, 7c, and 7d show the crack initiation, crack propagation, final fracture areas of AZ91, AZE911, AZ91-T6, and AZE911-T6, respectively. These areas are marked with numbers of 1, 2, and 3.

In Zone 1, cracks initiated by stresses (85MPa for AZ91, 125MPa for AZE911, 124.5MPa for AZ91-T6, and 176MPa for AZE911-T6) far below the yield stress

due to slippage, which resulted in a layered structure, with each protrusion and indents representing a cycle of tension and pressure. These cracks may be present in parts of the material due to dislocations. At this stage of fatigue failure, the second type of failure was shaped like the surface of a pearl. In Zone 2, the primary cracks grew enough to be able to grow with an acceptable stress concentration in a specific direction, perpendicular to the applied stress (85MPa for AZ91, 125MPa for AZE911, 124.5MPa for AZ91-T6, and 176MPa for AZE911-T6). In Zone 3, due to the high growth of cracks, the stress concentration was so high that it caused the plastic deformation of the material and the sudden fracture failure in the material. Finally, as a general comment, due to cleavage planes, the fracture behavior of the material was in a brittle mode in all studied cases.

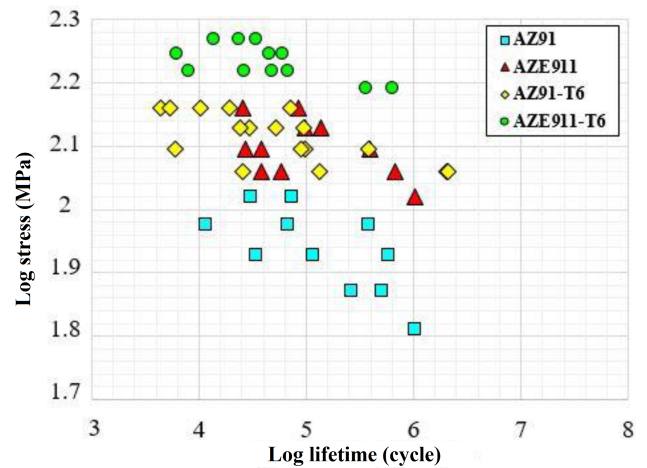


Fig. 6. The logarithmic value of the stress and the fatigue lifetime for all studied materials.

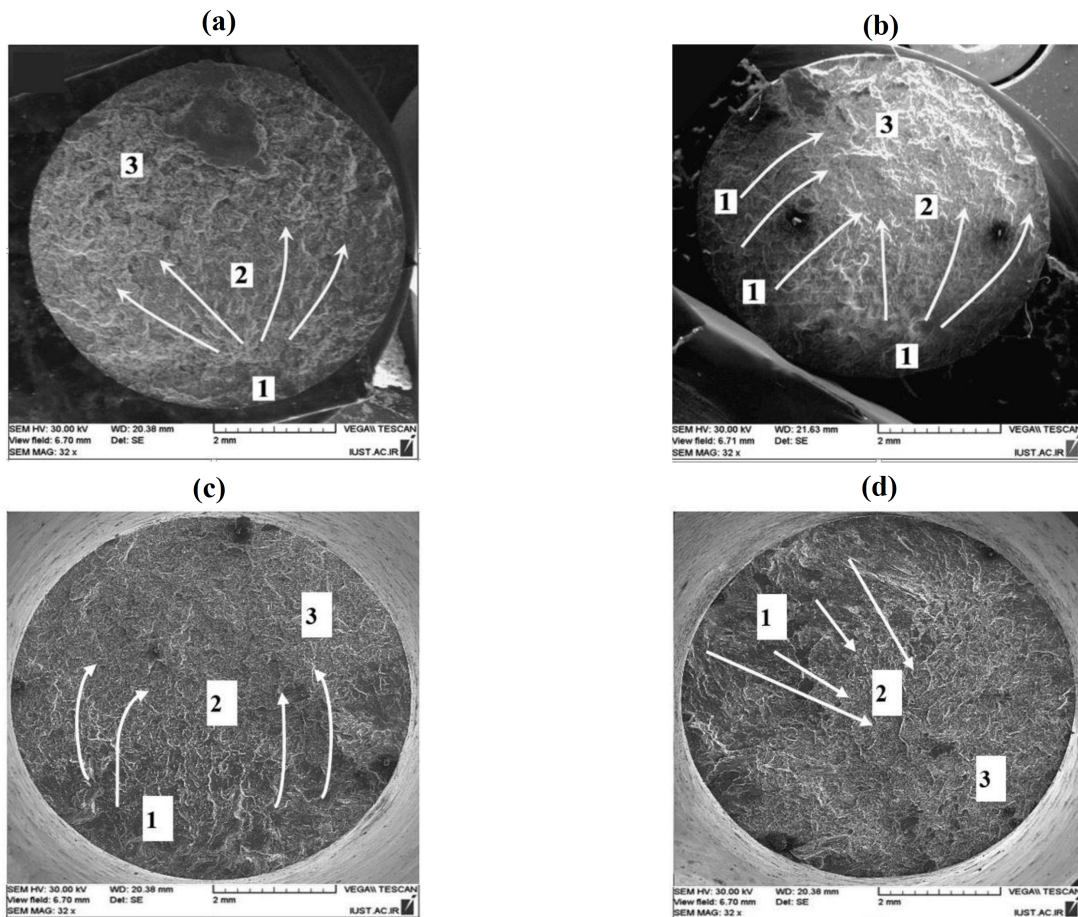


Fig. 7. The overview of the sample surface fracture for a) AZ91 at 85MPa, 581250 cycles, b) AZE911 at 125MPa, 386125 cycles, c) AZ91-T6 at 124.5MPa, 6000 cycles, and d) AZE911-T6 at 176MPa, 6100 cycles.

As a result, heat-treating and the addition of RE elements could improve the fatigue properties of magnesium alloys. Moreover, there are several methods for such an improvement in material behavior. One is the fabrication of the composite material with reinforcing particles: B_4C [41, 42], TiO_2 [43], ZrO_2 [43], and SiO_2

[33, 35, 36], with the powder metallurgy or stir-casting of light alloys. These reinforcements could increase the corrosion, quasi-static and dynamic mechanical properties, the wear and tensile behaviors of magnesium alloys.

4. Conclusions

In this research, the sensitivity analysis of the fatigue lifetime for the AZ91 magnesium alloy was carried out, in order to understand the effects of the heat treatment, the stress level, and the Rare-Earth (RE) element, under stress-controlled cyclic loading through High-Cycle Fatigue (HCF) regimes. The obtained results for this sensitivity analysis are mentioned as follows,

1. The RE element addition increased the material strength (the stress level) by at least 30%, at the same fatigue lifetime. However, both heat-treating and the RE element enhanced the strength by at least 50%, compared to the base material.
2. Based on the sensitivity analysis, the stress level, heat-treating, and the RE element were the most effective parameters on the fatigue lifetime of the AZ91 magnesium alloy, respectively.
3. The fatigue lifetime was also sensitive to the interaction of the heat treatment and the addition of the RE element into the base material.
4. According to the fracture surface of broken samples, three zones were detected for the crack initiation, the crack growth, and the sudden final fracture. Moreover, the fracture behavior of the studied materials was brittle due to the cleavage marks.

References

- [1] Z. Trojanová, P. Palček, M. Chalupová, P. Lukáč, I. Hlaváčová, High-frequency cycling behavior of three AZ magnesium alloys-microstructural characterization, *Int. J. Mater. Res.*, 107(10) (2016) 903-914.
- [2] L. Zhang, Q. Wang, W. Liao, W. Guo, B. Ye, H. Jiang, W. Ding, Effect of homogenization on the microstructure and mechanical properties of the repetitive-upsetting processed AZ91D alloy, *J. Mater. Sci. Technol.*, 33(9) (2017) 935-940.
- [3] P.H. Manrique, J.D. Robson, M.T. Pérez-Prado, Precipitation strengthening and reversed yield stress asymmetry in Mg alloys containing rare-earth elements: A quantitative study, *Acta Mater.*, 124 (2017) 456-467.
- [4] Y. Wang, G. Liu, Z. Fan, A new heat treatment procedure for rheo-diecast AZ91D magnesium alloy, *Scr. Mater.*, 54(5) (2006) 903-908.
- [5] H.Y. Wu, C.C. Hsu, J.B. Won, P.H. Sun, J.Y. Wang, S. Lee, C.H. Chiu, S. Torng, Effect of heat treatment on the microstructure and mechanical properties of the consolidated Mg alloy AZ91D machined chips, *J. Mater. Process. Technol.*, 209(8) (2009) 4194-4200.
- [6] A.M. Majd, M. Farzinfar, M. Pashakhanlou, M.J. Nayyeri, Effect of RE elements on the microstructural and mechanical properties of as-cast and age hardening processed Mg-4Al-2Sn alloy, *J. Magnesium Alloys*, 6(3) (2018) 309-317.
- [7] J.K. Kim, S.H. Oh, K.C. Kim, W.T. Kim, D.H. Kim, Effect of ageing time and temperature on the ageing behavior in Sn containing AZ91 alloy, *Met. Mater. Int.*, 23(2) (2017) 308-312.
- [8] Z. Li, A.A. Luo, Q. Wang, H. Zou, J. Dai, L. Peng, Fatigue characteristics of sand-cast AZ91D magnesium alloy, *J. Magnesium Alloys*, 5(1) (2017) 1-12.
- [9] S. Khisheh, K. Khalili, M. Azadi, V. Zaker Hendobadi, Heat treatment effect on microstructure, mechanical properties and fracture behavior of cylinder head aluminum-silicon-copper alloy, *J. Engine Res.*, 50 (2018) 55-65.
- [10] P. Zhang, Z. Li, H. Yue, Strain-controlled cyclic deformation behavior of cast Mg-2.99Nd-0.18Zn-0.38Zr and AZ91D magnesium alloys, *J. Mater. Sci.*, 51 (2016) 5469-5486.
- [11] M. Kuffova, Fatigue Endurance of Magnesium Alloys, A Chapter Book in Magnesium Alloys - Design, Processing and Properties, Edited by F. Czerwinski, IntechOpen Publication, (2011).
- [12] M. Azadi, M. Azadi, A. Hajiali Mohammadi, Effects of ageing and forging on short-term creep behaviors of Inconel-713C superalloy at 850°C, *Int. J. Eng.*, 33(4) (2020) 639-646.
- [13] P. Cavaliere, P.P. De Marco, Fatigue behavior of friction stir processed AZ91 magnesium alloy produced by high pressure die casting, *Mater. Charact.*, 58(3) (2007) 226-232.
- [14] M. Krupiński, T. Tański, Prediction of mechanical properties of cast Mg-Al-Zn alloys, *Arch. Mater. Sci. Eng.*, 56(1) (2012) 30-36.
- [15] A. Bag, W. Zhou, Tensile and fatigue behavior of AZ91D magnesium alloy, *J. Mater. Sci.*, 20 (2001) 457-459.
- [16] M. Pokorný, C. Monroe, C. Beckermann, L. Bichler, C. Ravindran, Prediction of hot tear formation in a magnesium alloy Permanent mold casting, *Int. J. Metalcast.*, 2(4) (2008) 41-53.

- [17] A.R. Vaidya, J.J. Lewandowski, Effects of SiCp size and volume fraction on the high cycle fatigue behavior of AZ91D magnesium alloy composites, *Mater. Sci. Eng., A*, 220(1-2) (1996) 85-92.
- [18] X.L. Xu, K. Zhang, X.G. Li, J. Lei, Y.S. Yang, T.J. Luo, High cycle fatigue properties of die-cast magnesium alloy AZ91D-1%MM, *Trans. Nonferrous Met. Soc. China*, 18(1) (2008) s306-s311.
- [19] Y. Yang, Y. Liu, S. Qin, Y. Fang, High cycle fatigue properties of die-cast magnesium alloy AZ91D with addition of different concentrations of cerium, *J. Rare Earths*, 24(5) (2006) 591-595.
- [20] Y. Yang, X. Li, Influence of neodymium on high cycle fatigue behavior of die-cast AZ91D magnesium alloy, *J. Rare Earths*, 28 (3) (2010) 456-460.
- [21] M. Mokhtarishirazabad, S.M.A. Boutorabi, M. Azadi, M. Nikravan, Effect of rare earth elements on high cycle fatigue behavior of AZ91 alloy, *Mater. Sci. Eng., A*, 587 (2013) 179-184.
- [22] C. Vanaret, P. Seufert, J. Schwientek, G. Karpov, G. Ryzhakov, I. Oseledets, N. Asprion, M. Bortz, Two-phase approaches to the optimal model-based design of experiments: how many experiments and which ones?, *Comput. Chem. Eng.*, 146 (2021) 107218.
- [23] K. Kumari, S. Yadav, Linear regression analysis study, *J. Pract. Cardiovasc. Sci.*, 4(1) (2018) 33-36.
- [24] B. Wolf, C. Fleck, D. Eifler, Characterization of the fatigue behavior of the magnesium alloy AZ91D by means of mechanical hysteresis and temperature measurements, *Int. J. Fatigue*, 26 (2004) 1357-1363.
- [25] D.K. Xu, E.H. Han, Effect of yttrium content on the ultra-high cycle fatigue behavior of Mg-Zn-Y-Zr alloys, *Mater. Sci. Forum*, 816 (2015) 333-336.
- [26] D.G.L. Prakash, D. Regener, W.J.J. Vorster, Effect of long-term annealing on the microstructure of HPDC AZ91 Mg alloy: A quantitative analysis by image processing, *Comput. Mater. Sci.*, 43(4) (2008) 759-766.
- [27] C. Suman, Heat treatment of magnesium die casting alloys AZ91D and AM60B, *SAE Tech. Pap.*, (1989) 890207.
- [28] Z.M. Li, Q.G. Wang, A.A. Luo, L.M. Peng, P.H. Fu, Y.X. Wang, Improved high cycle fatigue properties of a new magnesium alloy, *Mater. Sci. Eng., A*, 582 (2013) 170-177.
- [29] Y. Yang, H. Wu, Z.F. Xuan, Effect of solid solution treatment on fatigue behavior of cast magnesium alloy, *Appl. Mech. Mater.*, 281 (2013) 436-440.
- [30] A. Němcová, J. Zapletal, T. Podrábský, Fatigue behavior of AZ91 magnesium alloy, *Mech. Ser.*, 55(3) (2009) 141-147.
- [31] M. Mokhtarishirazabad, M. Azadi, G.H. Farrahi, G. Winter, W. Eichlseder, Improvement of high temperature fatigue lifetime in AZ91 magnesium alloy by heat treatment, *Mater. Sci. Eng., A*, 588 (2013) 357-365.
- [32] A.M. Afsari Golshan, H. Aroo, M. Azadi, Sensitivity analysis for effects of heat treatment, stress, and temperature on AlSi12CuNiMg aluminum alloy behavior under force-controlled creep loading, *Appl. Phys. A*, 127(1) (2021) 48.
- [33] M. Azadi, H. Aroo, Bending cyclic behavior and scatter-band analysis of aluminum alloys under beneficial and detrimental conditions through high cycle fatigue regime, *Frat. ed Integrita Strutt.*, 15(58) (2021) 272-281.
- [34] H. Aroo, M.S. Aghareb Parast, M. Azadi, M. Azadi, Investigation of effects of nano-particles, heat treatment process and acid amount on corrosion rate in piston aluminum alloy using regression analysis, 11th International Conference on Internal Combustion Engines and Oil (SAPCO), Tehran, Iran, (2020).
- [35] M. Azadi, M. Zomorodipour, A. Fereidoon, Sensitivity analysis of mechanical properties and ductile/brittle behaviors in aluminum-silicon alloy to loading rate and nano-particles, considering interaction effects, *Eng. Rep.*, 3(6) (2021) e12341.
- [36] M. Azadi, A. Naderi, A. Freidoon, Investigation of effects of the temperature and adding nano-SiO₂-particles on high-temperature mechanical properties for the piston aluminum-silicon alloy, *Iran. J. of Manuf. Eng.*, 8(3) (2021) 47-58 (In Persian).
- [37] S. Safarloo, F. Loghman, M. Azadi, M. Azadi, Optimal design experiment of ageing time and temperature in Inconel-713C superalloy based on hardness objective, *Trans. Indian Inst. Met.*, 71(3) (2018) 1563-1572.
- [38] S. Ishihara, S. Yoshifuji, T. Namito, T. Goshima, On the distributions of fatigue lives and defect-sizes in the die-cast magnesium alloy AZ91, *Procedia Eng.*, 2(1) (2010) 1253-1262.
- [39] H. Mayer, M. Papakyriacou, B. Zettl, S.E. Stanzl-Tschegg, Influence of porosity on the fatigue limit of die-cast magnesium and aluminum alloys, *Int. J. Fatigue*, 25 (2003) 245-256.

- [40] N. Fisch, E. Camp, K. Shertzer, R. Ahrens, Assessing likelihoods for fitting composition data within stock assessments, with emphasis on different degrees of process and observation error, *Fish. Res.*, 243 (2021) 106069.
- [41] K. Rahmani, G.H. Majzoubi, H. Bakhtiari, A. Sadooghi, On the effect of compaction velocity, size, and content of reinforcing particles on corrosion resistance of Mg-B₄C composites, *Mater. Chem. Phys.*, 271 (2021) 124946.
- [42] K. Rahmani, G.H. Majzoubi, G. Ebrahim-Zadeh, M. Kashfi, Comprehensive study on quasi-static and dynamic mechanical properties and wear behavior of Mg-B₄C composite compacted at several loading rates through powder metallurgy, *Trans. Nonferrous Met. Soc. China*, 31(2) (2021) 371-381.
- [43] K. Rahmani, A. Nouri, G. Wheatley, H. Malek-mohammadi, H. Bakhtiari, V. Yazdi, Determination of tensile behavior of hot-pressed Mg-TiO₂ and Mg-ZrO₂ nanocomposites using indentation test and a holistic inverse modeling technique, *J. Mater. Res. Technol.*, 14 (2021) 2107-2114.